A Platinum Open Access Journal for Organic Chemistry

Paper

Free to Authors and Readers

DOAJ Seal

Arkivoc **2025**, part __, 0-0

to be inserted by editorial office

Benzyltriethylammonium chloride (BTEAC) catalyzed efficient synthesis of novel benzofuran-pyrazole hybrids: design, synthesis and in silico evaluation as potential anti-HCV agents

Aqsa Mushtaq and Ameer Fawad Zahoor*

Department of Chemistry, Government College University Faisalabad, 38000-Faisalabad, Pakistan
Email: fawad.zahoor@gcuf.edu.pk

Received mm-dd-yyyy **Accepted** mm-dd-yyyy **Published on line** mm-dd-yyyy

Dates to be inserted by editorial office

Abstract

An efficient and green protocol has been developed by treating substituted benzofuran-based hydrazides with acetylacetone using benzyltriethylammonium chloride (BTEAC) under neat conditions to afford novel benzofuran-pyrazole hybrids in moderate to excellent yields (56-90%). The structures of synthesized derivatives were validated via different spectroscopic techniques. Taking into consideration the integral roles of NS5A and NS5B in the life cycle of HCV, the prepared set of hybrids was also evaluated via molecular docking analysis against these two non-structural protein targets.

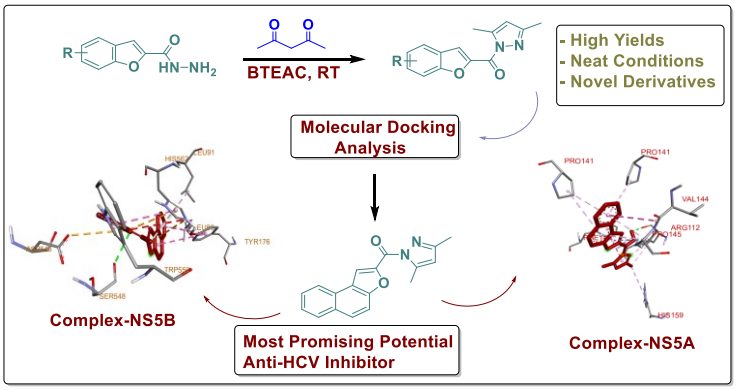

Keywords: BTEAC, efficient protocol, benzofuran-pyrazole hybrids, anti-HCV

Introduction

Heterocyclic compounds are usually considered to be the foundation of the pharmaceutical industry as several commonly employed drugs constitute diverse heterocyclic frameworks[1]. The nitrogen and oxygen containing heterocyclic functionalities correspond to the key components in drug development[2]. Pyrazole is a five-membered and two nitrogen containing heterocyclic ring which is commonly found in several pharmaceuticals, biologically active natural products and agrochemicals[3]. Diverse synthetic routes have been developed for the construction of the pyrazole nucleus and its derivatives which involve the coupling reaction of hydrazine, ethyl acetoacetate and aldehyde[4], reaction of hydrazines and chalcones[5] and Suzuki-Miyaura cross coupling reaction[6]. The developed protocols involve the utilization of magnetic Fe_3O_4 nanoparticles[7], Amberlyst A-21[8], choline chloride urea (deep eutectic solvent (DES))[9], DABCO[10], MgO nanoparticles[11], β-cyclodextrin-SO_3H[12], Et_3N[13], sodium benzoate[14], sodium bromide[15], trichloroacetic acid[16], isonicotinic acid[17] and [Hmim][HSO_4][18] etc. In addition, L-proline[19], Mg/Al hydrotalcite[20] and (aqueous) PEG-400[21] have also been harnessed towards the formation of several pyrazole derivatives. The preferred choice for constructing the pyrazole core involves the reaction of hydrazines with 1,3-dicarbonyl compound using acid as catalyst. Regarding this, several acids i.e., sulfuric acid[22], polystyrene-substituted sulfonic acid[23], citric acid[24], silica supported sulfuric acid[25] and various others have been harnessed to furnish the targeted pyrazole-based organic molecules. However, most of these developed approaches have been found to suffer from several limitations including long reaction times, use of non-ecofriendly solvents, expensive catalysts, inadequate yields and arduous purification techniques. Thus, these factors highlight the requirement of developing a novel and facile catalytic synthetic route for the construction of pyrazole nucleus to overcome these challenges.

Organic molecules incorporated with pyrazole nucleus are known to illustrate a wide array of biological properties which include anti-viral[26], anti-fungal[27], anti-cancer[28] and anti-bacterial activities[29] Moreover, pyrazole based organic compounds have also been utilized as effective pain killer[30], inflammation alleviator[31], stress buster agents[32]. Figure 1 illustrates the structures of some commonly employed pyrazole scaffold containing drugs[32]. Furthermore, oxygen atom containing benzofuran scaffolds have been known to display extensive pharmacological properties, thereby highlighting their significance in chemical pharmacology[33] Diverse natural and synthetic benzofuran derivatives illustrate varied medicinal properties and have been investigated thoroughly to act as potential anti-mitotic[34], anti-bacterial[35], anti-arrhythmic[36], anti-viral[37], and anti-tyrosinase agents[38,39]. For example, saprisartan **4** and psoralen **5** are benzofuran endowed drugs which have been determined to be effective against hypertension and skin diseases respectively (Figure 1)[40]. Considering the therapeutical significance of pyrazole and benzofuran scaffolds, researchers have been endeavoring to develop medicinally active organic molecules endowed with these heterocyclic frameworks. For instance, benzofuran tethered pyrazole-pyridine hybrid **6**[41], phenyl linked benzofuran-pyrazole hybrid **7**[42] and biphenyl-benzofuran-pyrazole hybrid **8**[43] exhibit promising bioactivities against osteoarthritis, microbes and α-glucosidase, respectively (Figure 1).

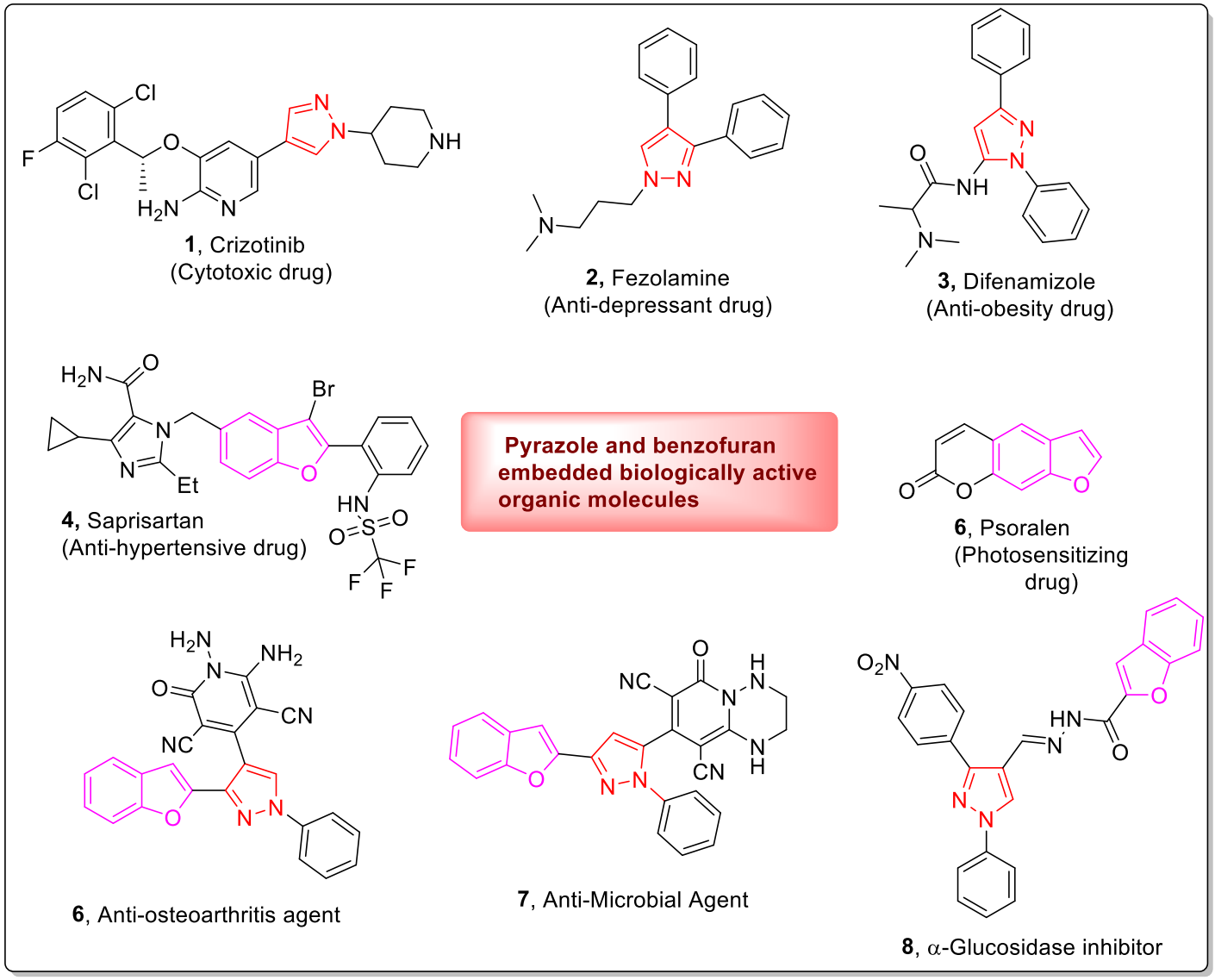

Figure 1. Structures of some pyrazole and benzofuran constituting biologically active organic compounds.

Here, we have established a novel and facile synthetic protocol involving the use of easily accessible catalyst i.e., BTEAC in environmentally benign conditions to afford the pyrazole derivatives in high yields within short duration. For this purpose, benzofuran-endowed substrates (hydrazides) were reacted with acetylacetone using novel synthetic protocol to access a new series of benzofuran-pyrazole hybrids.

To determine the biological potential of synthesized benzofuran-pyrazole hybrids **11(a-j)** as anti-HCV agents, molecular docking analysis was carried out by targeting these novel derivatives with the significant non-structural proteins of HCV i.e., NS5A and NS5B. These protein targets were selected on the basis of their essential roles within the life cycle of HCV. The potent derivatives were further subjected to ADMET evaluation to get insights about their absorption, distribution, metabolism, excretion and toxicity parameters.

Results and Discussion

Synthesis: The substituted benzofuran-based hydrazides **9(a-j)** were synthesized through developed protocol in reasonable yields[44]. In order to carry out the synthesis of pyrazole derivatives, 5-bromobenzofuran-based hydrazide **9a** was chosen as a model substrate and was allowed to react with acetyl acetone **10** in the presence of several catalysts under different conditions. Initially, the reaction between hydrazide **9a** and acetyl acetone **10** was carried out using catalytic amount of sulfuric acid in water at room temperature, which resulted in low yield (35%) of targeted pyrazole derivative **11a** in 45 minutes (Table 1, entry 1). Upon carrying out the reaction at 80 °C, 30% yield was obtained in 30 minutes (Table 1, entry 2). However, slightly better yield (45%) was attained (in 30 minutes) under solvent-free conditions at room temperature (Table 1, entry 3). This reaction was further investigated using different amino acids (i.e., glycine, L-cysteine and L-proline) as catalysts under a variety of conditions which resulted in low to moderate yields (37-65%) of benzofuran-pyrazole derivative **11a** within 30-55 minutes (Table 1, entries 4-10). In addition, curd water was also employed to determine its catalytic effect in solvent-free conditions, which gave 62% yield at 60 °C and 65% yield at room temperature (Table 1, entries 11 & 13). Furthermore, catalytic role of dried eggshell powder was also explored under aqueous (at 60 °C) and solvent free conditions (at room temperature), which afforded targeted benzofuran-pyrazole hybrid in 38% and 40% yield respectively (Table 1, entries 12 & 14). Similarly, trichloro acetic acid mediated model reaction afforded **11a** in 70% yield under neat conditions (Table 1, entry 15). This model reaction was also carried out by using BTEAC in methanol at 80 °C and at RT that afforded the target molecule in higher yields i.e., 70% (20 min) and 75% (25 min), correspondingly (Table 1, entries 16 & 17). However, when the reaction was proceeded using BTEAC under neat conditions, excellent yield (88%) of target molecule **11a** was achieved after 20 minutes (Table 1, entry 18).

Table 1. Optimization of reaction conditions[a]

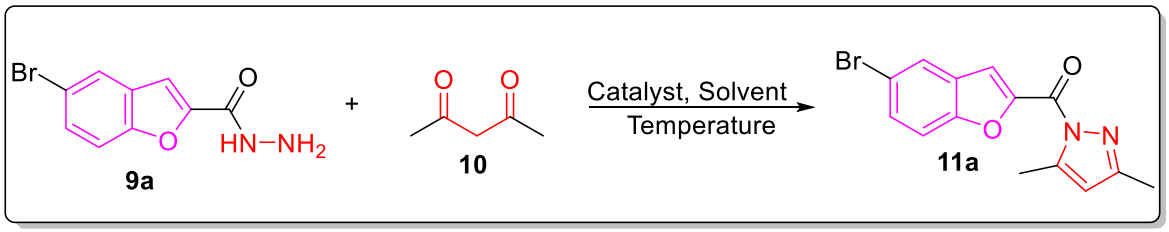

Sr. No.	Catalyst	Solvent	Temperature	Time	Yield
1	H_2SO_4	H_2O	RT	45 min	35%
2	H_2SO_4	H_2O	80 °C	30 min	30%
3	H_2SO_4	Solvent-free	RT	30 min	45%
4	Glycine	H_2O	RT	35 min	55%
5	Glycine	H_2O	80 °C	30 min	51%
6	L-Cysteine	EtOH	RT	45 min	45%
7	L-Cysteine	EtOH	80 °C	40 min	41%
8	L-Proline	MeOH	RT	55 min	40%
9	L-Proline	MeOH	70 °C	50 min	37%
10	Glycine	Solvent-free	RT	35 min	65%
11	Curd water	Solvent-free	60 °C	40 min	62%
12	Dried egg shell powder	H_2O	60 °C	45 min	38%

13	Curd water	Solvent-free	RT	45 min	65%
14	Dried egg shell powder	Solvent-free	RT	50 min	40%
15	Cl_3CCOOH	Solvent-free	RT	30 min	70%
16	BTEAC	MeOH	80 ^oC	20 min	70%
17	BTEAC	MeOH	RT	25 min	75%
18	BTEAC	Solvent-free	RT	20 min	88%

[a]Reaction Conditions: **9a** (1 mmol), **10** (3 mmol), catalyst (10 mol %), RT: Room Temperature

In order to check the substrate scope of the developed protocol, substituted benzofuran-based hydrazides **9(a-j)** were allowed to react with acetylacetone **10** under optimized conditions to afford a novel library of benzofuran-pyrazole hybrids **11(a-j)** in high yields (72-90%). Diversely substituted substrates (benzohydrazides) were utilized in the newly developed protocol. The benzofuran-based hydrazides substituted with electron donating groups (OMe, OEt, Me), electron withdrawing groups (Br and Cl) and aryl fused substituted substrates were harnessed in optimized conditions to result in efficient yields (76-88%) of target molecules. Meanwhile, unsubstituted benzofuran-pyrazole derivative **11c** and naphthofuran endowed derivative **11d** were attained in 72% and 83% yield, respectively. The electron donating groups (OMe, OEt, Me), substituted substrates afforded the corresponding target molecules **11e**-**11h** in 75-90% yield range. while electron withdrawing groups (Br and Cl) substituted substrates furnished the desired hybrids (**11a**, **11b** & **11i**) in 78-88% yield range. It was inferred that the position of substituents had no significant effect on the yield of target molecules with an exception of nitro-substituted benzofuran-pyrazole hybrid **11j**. The strongly electron withdrawing (-NO_2) group substituted benzofuran-pyrazole hybrid **11j** was achieved in relatively moderate yield i.e., 56% (Scheme 1).

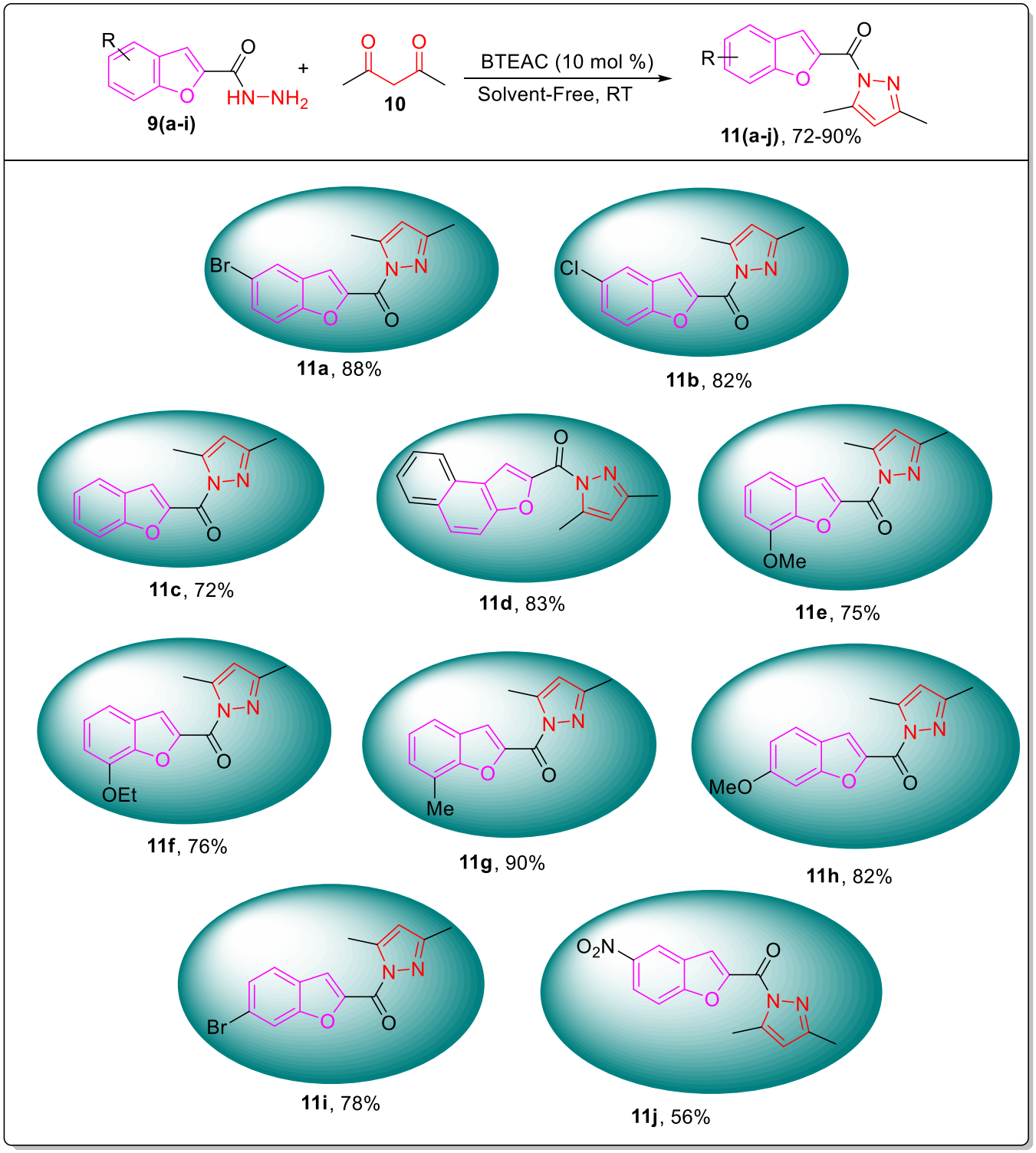

Scheme 1: Synthesis of benzofuran-pyrazole derivatives **11(a-j)** under optimized conditions

The mechanism for the developed BTEAC catalyzed synthesis of pyrazoles may be postulated as illustrated in Figure 2. Initially, the condensation of benzofuran-based hydrazide **9a** with acetylacetone **10** results in the formation of corresponding imine **I**. Subsequently, the chloride ion of BTEAC possibly abstracts the proton from the NH of imine, thereby facilitating its attack on the activated carbonyl carbon (via potential coordination with benzyl triethylammonium cation) to generate intermediate **II**. The intermediate **II** further gets transformed to required benzofuran-pyrazole hybrid **11a** upon dehydration (Figure 2).

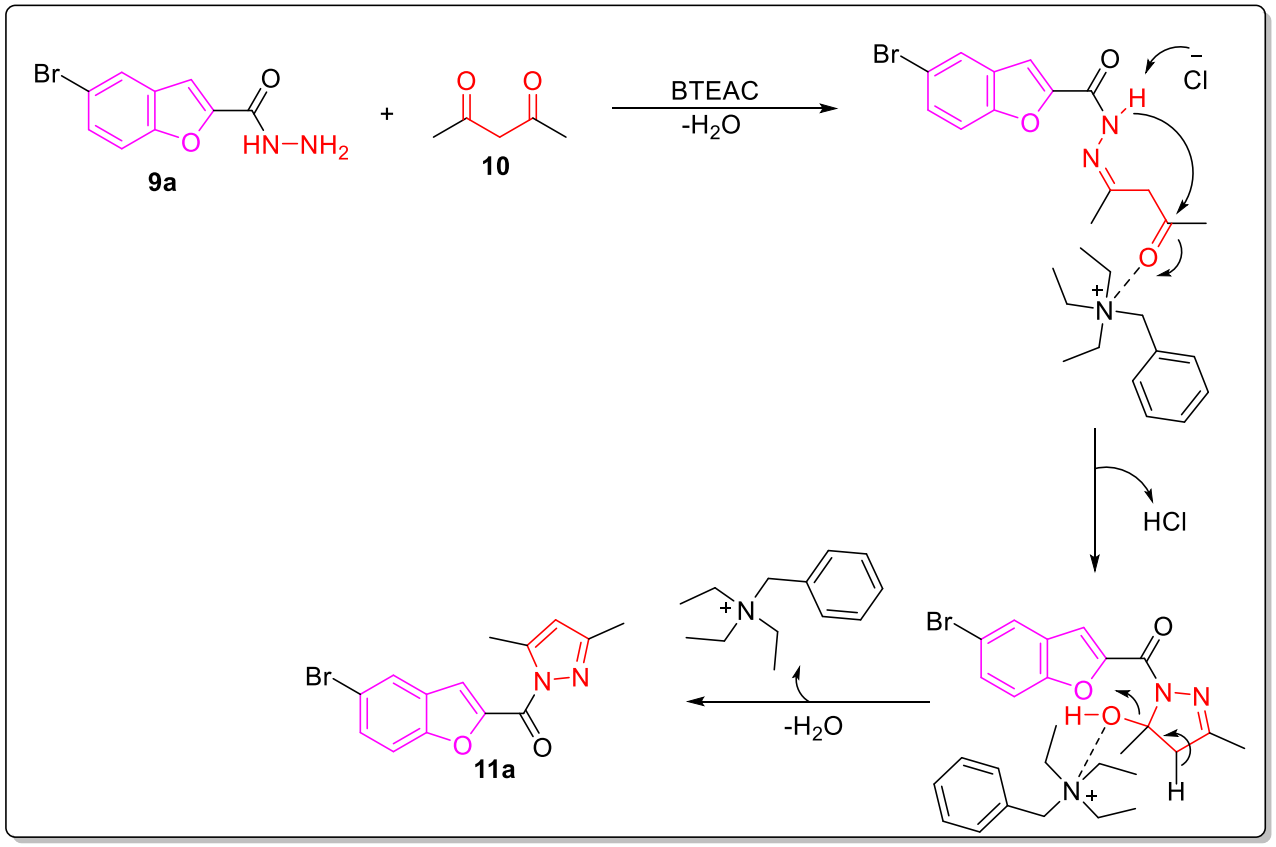

Figure 2. Plausible mechanism for the synthesis of benzofuran-pyrazole hybrids.

The structures of synthesized benzofuran-pyrazole derivatives **11(a-e)** were authenticated via NMR spectroscopy, mass spectrometry and elemental analysis. The ^{1}H-NMR spectrum of derivative **11a** illustrates the two singlet peaks (at 2.31 and 2.63 ppm) of two methyl groups substituted on the pyrazole ring. In addition, a singlet peak of one proton at 6.06 ppm indicates the signal of pyrazole-H. In addition, the signals of aromatic protons were observed within 7.44-8.23 ppm, with a singlet peak of furan proton at 7.86 ppm. In a similar manner, within the ^{13}C-NMR spectrum of **11a**, two peaks of two methyl carbons were observed at 13.9 and 14.5 ppm. Moreover, the unsubstituted carbon of pyrazole ring was observed to give signal at 111.4 ppm. In addition, another characteristic peak of carbonyl carbon was determined to be at 153.3 ppm. The molecular weight of the compound **11a** was determined by the presence of molecular ion peak at m/z 318.9 [M^{+}]. In addition, the percentage of carbon, hydrogen and nitrogen was found to be close to the calculated value, via elemental analysis. All of the synthesized pyrazole-benzofuran derivatives were characterized in the similar manner (Supplementary material file).

Molecular docking Analysis with NS5A

NS5A protein of HCV has been considered as persuasive target owing to its diverse and multifunctional role in the HCV life cycle[45]. All of the newly synthesized novel hybrids were subjected to molecular docking analysis against NS5A target of HCV to determine their potency as anti-HCV agents. All of the newly prepared derivatives were found to be efficient inhibitors as evaluated by their interaction types and docking scores

which were found to be in the range of -8.7 to -10.6 Kcal/mol (Table 2 & Table S1). The binding score and resulting interactions unveiled the significant and remarkable potency of **11d** (-10.6 Kcal/mol) among all the synthesized hybrids and employed standards i.e., daclatasvir (-10.4 Kcal/mol), GSK-2336805 (-9.6 Kcal/mol), and ABT-267 (-8.2 Kcal/mol). Meanwhile, derivative **11b** was also determined to be efficient HCV-inhibitor as its binding score -9.1 Kcal/mol was found to be more promising than standard ABT-267 and comparable with GSK-2336805 (Figure S21 & S22).

Table 2. Molecular docking analysis of synthesized benzofuran-pyrazole derivatives **11(a-i)** within the active site of NS5A

Sr. No.	Compound	Docking Score (Kcal/mol)
1	**11a**	-8.8
2	**11b**	-9.1
3	**11c**	-8.4
4	**11d**	-10.6
5	**11e**	-8.9
6	**11f**	-8.8
7	**11g**	-8.9
8	**11h**	-8.8
9	**11i**	-8.7
10	**11j**	-9.0
11	Daclatasvir	-10.4
12	GSK-2336805	-9.6
13	ABT-267	-8.2

The aromatic rings of napthofuran scaffold within the **11d** elicited multiple hydrophobic interactions which include amide-pi stacked interactions with Val 144 (4.77 Å) and several pi-alkyl interactions with Pro 145 and Pro 141. The carbonyl oxygen atom of this promising inhibitor was found to display conventional hydrogen bonding interactions with Arg 112 at a bond distance of 2.47 Å. The pyrazole framework of the **11d** also established pi-pi T-shaped, pi-alkyl and alkyl type hydrophobic interactions with Phe 149, Arg 112, His 159, and Arg 112 residues (Figure 3). For compound **11b**, the aromatic rings of benzofuran scaffold were observed to form two pi-cation type electrostatic interactions with His 159 at 4.29 Å and 3.94 Å bond distances. Other pi-cation type electrostatic interactions were observed between pyrazole ring and His 159 (3.78 Å). Moreover, **11b** was also found to be engaged in several hydrophobic interactions including pi-pi stacked, alkyl and pi-alkyl interactions with Arg 160, Pro 100, Tyr 161 and His 159 amino acid residues (Figure S21).

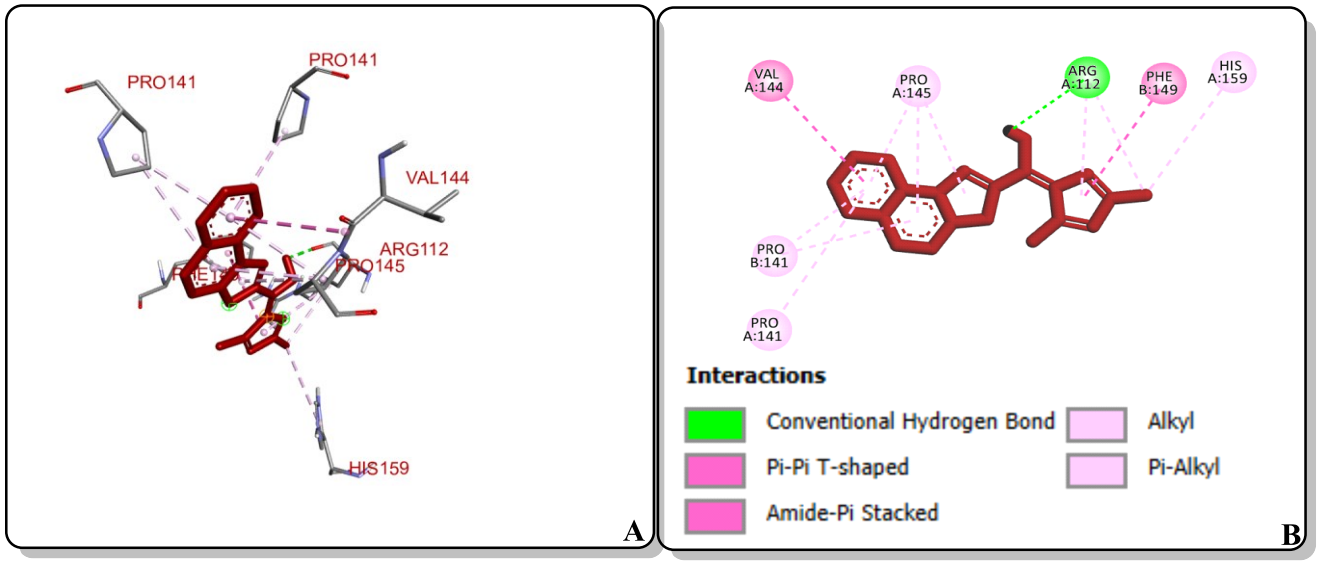

Figure 3. Binding interactions of derivative **11d** with NS5A. A) Interactions of best docked pose of ligand **11d** with protein NS5A B) 2D-Interactions between **11d** and NS5A.

Molecular Docking studies with NS5B

NS5B is another nonstructural protein of HCV which has been found to constitute RdRp (RNA dependent RNA polymerase), thereby playing an indispensable role towards its replication[46]. Molecular docking analysis was also carried out by subjecting all of the synthesized benzofuran-pyrazole hybrids **11(a-j)** against the NS5B protein target to assess the anti-HCV potential of synthesized hybrids. The in-silico analysis of synthesized hybrids and employed standards i.e., valopicitabine, VCH-759 and sofosbuvir triphosphate unveiled that all of the synthesized derivatives showcased significant anti-HCV potential by developing promising interactions within the binding site of targeted receptor. The promising interactions are attributed to their remarkable binding energies which were found to be in the range of -6.3 to -7.6 Kcal/mol, thereby illustrating effective inhibition potency with respect to utilized standards i.e., valopicitabine (-6.7 Kcal/mol), VCH-759 (-7.4 Kcal/mol) and sofosbuvir triphosphate (-7.1 Kcal/mol) (Table 3 & Table S2). Thus, the results interpreted the **11d** as the most promising target as indicated by its efficacious binding score (-7.6 Kcal/mol). Similarly, **11j** was determined to be second promising inhibitor among the synthesized hybrids as its binding score (-7.0 Kcal/mol) was observed to be more effective than standard valopicitabine and comparable to other two standards (Figure S23 & S24).

Table 3: Molecular docking analysis of synthesized benzofuran-pyrazole derivatives **11(a-i)** within the active site of NS5B

Sr. No.	Compound	Docking Score (Kcal/mol)
1	**11a**	-6.3
2	**11b**	-6.9
3	**11c**	-6.8
4	**11d**	-7.6
5	**11e**	-6.7
6	**11f**	-6.6

7	**11g**	-6.8
8	**11h**	-6.5
9	**11i**	-6.5
10	**11j**	-7.0
11	Sofosbuvir triphosphate	-7.1
12	Valopicitabine	-6.7
13	VCH-759	-7.4

The most potent inhibitor **11d** was analyzed to reveal several interactions with the NS5B target which constitute several electrostatic, hydrogen bonding and hydrophobic interactions. The aromatic rings of naphthyl functionality established pi-pi T-shaped and pi-alkyl type hydrophobic interactions with Tyr 176, Leu 91 and Leu 83 residues. In addition, one of the nitrogen atoms of pyrazole ring was found to be engaged in conventional hydrogen bonding interactions with Ser 548 (dHB = 2.72 Å). Besides these interactions, **11d** also established pi-donor hydrogen bonding, attractive charge type electrostatic interactions, pi-pi stacked, pi-cation and pi-alkyl type hydrophobic interactions with His 562, Tyr 176, Asp 546, and Trp 550 (Figure 4). In case of **11j**, both oxygen atoms of nitro group developed conventional H-bonding interactions with Arg 254 (dHb = 2.71 Å) and Arg 250 (dHb = 1.99 Å). The pyrazole core and benzofuran cores of the hybrid **11j** were determined to be involved in electrostatic interactions i.e., pi-cation and pi-anion interaction with Lys 79 and Asp 244. In addition, Arg 234, Val 235 and Pro-247 amino acid residues also illustrated pi-sigma and pi-alkyl type hydrophobic interactions with benzofuran scaffold (Figure S23).

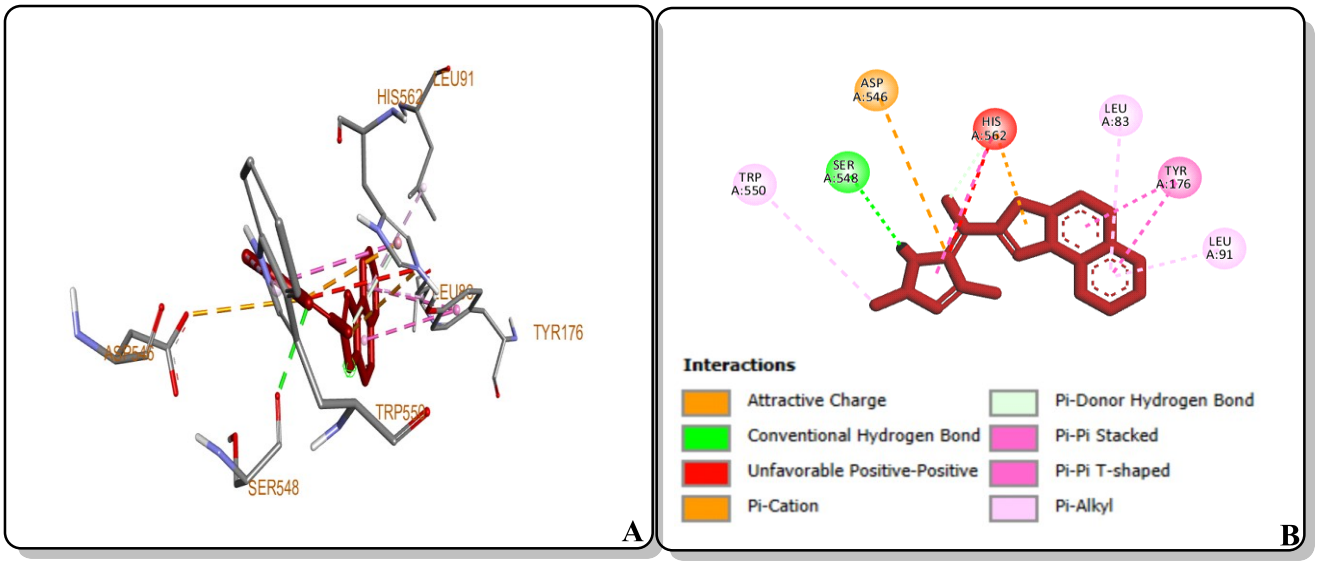

Figure 4: Binding interactions of derivative **11d** with NS5B. (A) Interactions of best docked pose of ligand **11d** with protein NS5B. (B) 2D-Interactions between **11d** and NS5B.

ADMET Analysis

The analysis of physiochemical properties of potent synthesized pyrazole derivatives (**11b**, **11d** and **11j)** and corresponding standards (i.e., daclatasvir and VCH-759) unveiled the acceptance of Lipinski's rule for all compounds except standard daclatasvir. The intestinal absorption of compound is evaluated via Caco-2

permeability score whose optimal value is considered to be above -5.15. Thus, in this regard, Caco-2 permeability score was found to be optimal for chosen synthesized hybrids in comparison to chosen standards. HIA values were also determined to be efficacious for all of them. In addition, the possibility of each compound to behave as Pgp-inhibitor is determined via its corresponding output value. Moreover, output values for VDss were analyzed to be within the optimal range i.e., 0.04-20 L/Kg for all compounds except for standard VCH-759, whose VDss output value was found to be -0.048 (Table S3).

The metabolism properties of chosen derivatives and standards revealed their probabilities to act as CYP2D6, CYP1A2, CYP3A4, CYP2C19, CYP2B6 and CYP2C9 inhibitors. Furthermore, the clearance rate of these compounds from plasma was evaluated via CL_{plasma} values, which indicated moderate clearance rate of analyzed compounds. Furthermore, potent compounds **11b** and **11d** exhibited low-moderate output values for AMES toxicity, eye corrosiveness, respiratory toxicity, human hepatotoxicity and rat oral acute toxicity, thereby indicating their safe pharmacokinetic profile. In comparison, potent hybrid **11j** was determined to be potentially toxic as indicated by its output values for AMES toxicity and respiratory toxicity. Furthermore, the output values of daclatasvir suggest its potential rat oral acute toxicity and AMES toxicity. Similarly, the VCH-759 was also found to be potentially human hepatotoxic via its respective output value (Table S3). Thus, overall interpretation of ADMET features of these compounds highlight the efficiency and significance of synthesized potent hybrids **11b** and **11d** in comparison to standard inhibitors.

Conclusions

To conclude, an efficacious and eco-friendly protocol has been developed by utilizing BTEAC as a catalyst in solvent-free conditions to afford a novel series of substituted benzofuran-pyrazole hybrids in moderate to efficient yields (56-90%) by treating acetylacetone with substituted benzofuran-based hydrazides. Relative spectroscopic analyses were carried out to confirm the structures of synthesized derivatives. High yields, facile accessibility of reagents, short reaction time and solvent-free conditions are some of the significant merits of the developed protocol. In addition, this study also reports the anti-HCV evaluation of novel substituted benzofuran-pyrazole hybrids. All of the synthesized derivatives displayed efficient interactions against the targeted receptors i.e., NS5A and NS5B. More significantly, naphthofuran-endowed derivative was unveiled as the most promising anti-HCV agent owing to its remarkable docking scores (-10.6 & -7.6 Kcal/mol) and efficient binding interactions in comparison to employed NS5A and NS5B standard inhibitors. Meanwhile, Cl and NO_2 substituted derivatives were also found to be potentially efficient anti-HCV agents due to their significant interactions with both targets. These promising synthesized derivatives were further subjected to ADMET evaluation, which unveiled the relatively safe pharmacokinetic profile of naphthofuran and chloro-substituted pyrazole hybrids. These in silico findings highlight the potential applicability of these potent benzofuran-pyrazole hybrids as effective anti-HCV agents for future preclinical studies.

Experimental Section

General. To accomplish the synthesis of novel pyrazole derivatives, all the required chemicals and solvents were purchased from Alfa Aesar (Lancashire, United Kingdom), Macklin (China, Shanghai Pudong New Area) and Honeywell (Charlotte, North Carolina). All the purchased chemicals were of analytical grade and were

employed as such without carrying out any purification strategy. Analysis of reaction's progress was done via TLC (thin layer chromatography). To infer the melting points of synthesized derivatives, WRS-1B melting point apparatus was utilized and uncorrected melting points were documented. ^{1}H-NMR spectra and ^{13}C-NMR spectra of prepared derivatives were recorded via Bruker spectrophotometer operating at 400 MHz/600 MHZ and 100 MHz/400 MHz, respectively. Deuterated dimethyl sulfoxide and deuterated chloroform were used as solvents. Meanwhile, TMS was chosen as internal standard. Spectral interpretation was carried out via MestReNova. Within the structural interpretation section, the listed abbreviations "s, d, t, q and m" stand for "singlet, doublet, triplet, quatret and multiplet" respectively. Denotation of coupling constant is done by symbol "J", whose value is given hertz (Hz).

Developed synthetic protocols

A mixture of substituted bezohydrazides **9(a-h)** (1 mmol), acetylacetone **10** (3 mmol) and BTEAC (10 mol %) was stirred at room temperature under neat conditions until the completion of reaction. Upon indication of reaction completion via TLC, solvent extraction was carried using ethyl acetate. The organic layer was dried over anhydrous sodium sulfate and the concentrate was further subjected to column chromatography to afford the target molecules in purified form.

(5-Bromobenzofuran-2-yl)(3,5-dimethyl-1*H*-pyrazol-1-yl)methanone (**11a**). Light brown solid, 88% yield, mp: 150-152 ^{o}C, ^{1}H-NMR (400 MHz, $CDCl_3$): δ 2.31 (s, 3H), 2.63 (s, 3H), 6.06 (s, 1H), 7.44-7.55 (m, 2H), 7.86 (s, 1H), 8.23 (s, 1H). ^{13}C NMR (100 MHz, $CDCl_3$) δ 13.9, 14.5, 111.4, 113.8, 116.7, 118.7, 125.9, 129.2, 131.0, 145.7, 147.2, 153.3, 154.2, 157.3. MS, *m/z*: 318.9 [M^+]. Anal. Calcd for $C_{14}H_{11}BrN_2O_2$: C, 52.69; H, 3.47; N, 8.78. Found: C, 52.77; H, 3.38; N, 8.58%.

(5-Chlorobenzofuran-2-yl)(3,5-dimethyl-1*H*-pyrazol-1-yl)methanone (**11b**). Off-white solid, 82%, mp: 141-143 ^{o}C, ^{1}H-NMR (600 MHz, DMSO-d6): δ 2.24 (s, 3H), 2.52 (s, 3H), 6.29 (s, 1H), 7.53-7.55 (m, 1H), 7.77-7.79 (m, 1H), 7.97 (s, 1H), 8.25 (s, 1H). ^{13}C NMR (150 MHz, DMSO-d6) δ 14.1, 14.6, 112.2, 114.3, 119.5, 123.8, 128.8, 129.0, 129.0, 145.5, 147.4, 153.4, 153.8, 156.9. MS, *m/z*: 274.2 [M^+]. Anal. Calcd for $C_{14}H_{11}ClN_2O_2$: C, 61.21; H, 4.04; N, 10.20. Found: C, 61.40; H, 4.02; N, 10.41%.

Benzofuran-2-yl(3,5-dimethyl-1*H*-pyrazol-1-yl)methanone (**11c**). Brown solid, 72% yield, mp: 110-112 ^{o}C, ^{1}H-NMR (600 MHz, DMSO-d6): δ 2.24 (s, 3H), 2.52 (s, 3H), 6.28 (s, 1H), 7.35 (t, *J* = 9 Hz, 1H), 7.51-7.54 (m, 1H), 7.73 (d, *J* = 6 Hz, 1H), 7.89 (d, *J* = 6 Hz, 1H), 8.31 (s, 1H). ^{13}C NMR (150 MHz, DMSO-d6) δ 14.1, 14.6, 112.0, 112.0, 112.5, 120.3, 124.6, 127.4, 129.0, 145.4, 146.1, 153.2, 155.4, 157.2. MS, *m/z*: 241.1 [M+1]$^+$. Anal. Calcd for $C_{14}H_{12}N_2O_2$: C, 69.99; H, 5.03; N, 11.66. Found: C, 69.79, H, 5.01; N, 11.30%.

(3,5-Dimethyl-1*H*-pyrazol-1-yl)(naphtho[2,1-*b*]furan-2-yl)methanone (11d). Light brown solid, 83% yield, mp: 152-154 ^{o}C, ^{1}H-NMR (600 MHz, DMSO-d6): δ 2.30 (s, 3H), 2.55 (s, 3H), 6.30 (s, 1H), 7.57-7.59 (m, 1H), 7.67-7.69 (m, 1H), 7.89 (d, *J* = 6 Hz, 1H), 8.04-8.08 (m, 2H), 8.46 (d, *J* = 12 Hz, 1H), 8.87 (s, 1H). ^{13}C NMR (150 MHz, DMSO-d6) δ 14.2, 14.6, 112.0, 113.1, 119.4, 123.1, 124.3, 126.2, 128.1, 128.4, 129.5, 130.6, 130.7, 145.3, 145.8, 153.2, 154.1, 157.1. MS, *m/z*: 291.0 [M+1]$^+$. Anal. Calcd for $C_{18}H_{14}N_2O_2$: C, 74.47; H, 4.86; N, 9.65. Found: C, 74.36; H, 4.88; N, 9.45%.

(3,5-Dimethyl-1*H*-pyrazol-1-yl)(7-methoxybenzofuran-2-yl)methanone (**11e**). Light yellow solid, 75%, mp: 108-110 ^{o}C, ^{1}H-NMR (600 MHz, DMSO-d6): δ 2.24 (s, 3H), 2.52 (s, 3H), 3.94 (s, 3H), 6.28 (s, 1H), 7.11 (d, *J* = 6 Hz, 1H), 7.26 (t, *J* = 9 Hz, 1H), 7.41 (d, *J* = 12 Hz, 1H), 8.28 (s, 1H). ^{13}C NMR (150 MHz, DMSO-d6) δ 14.1, 14.6, 56.4, 110.4, 112.0, 112.1, 116.0, 125.3, 129.0, 145.1, 145.4, 145.8, 146.1, 153.2, 157.1. MS, *m/z*: 271.0 [M+1]$^+$. Anal. Calcd for $C_{15}H_{14}N_2O_3$: C, 66.66; H, 5.22; N, 10.36. Found: C, 66.46; H, 5.24; N, 10.48%.

(3,5-Dimethyl-1*H*-pyrazol-1-yl)(7-ethoxybenzofuran-2-yl)methanone (**11f**). Light yellow solid, 76% yield, mp: 106-108 °C, ^{1}H-NMR (600 MHz, DMSO-d6): δ 1.40 (t, *J* = 6 Hz, 3H), 2.24 (s, 3H), 2.53 (s, 3H), 4.22 (q, *J* = 9 Hz, 2H), 6.29 (s, 1H), 7.10 (d, *J* = 6 Hz, 1H), 7.24 (t, *J* = 6 Hz, 1H), 7.40 (d, *J* = 12 Hz, 1H), 8.28 (s, 1H). ^{13}C NMR (150 MHz, DMSO-d6) δ 14.1, 14.6, 14.6, 64.7, 110.2, 111.2, 112.0, 115.9, 125.4, 129.0, 140.9, 141.5, 145.0, 145.5, 153.2, 157.2. MS, *m/z*: 268.9 $[M\text{-}CH_3]^+$. Anal. Calcd for $C_{16}H_{16}N_2O_3$; C, 67.59; H, 5.67; N, 9.85. Found: C, 67.57; H, 5.89; N, 9.81%.

(3,5-Dimethyl-1*H*-pyrazol-1-yl)(7-methylbenzofuran-2-yl)methanone (**11g**). White solid, 90% yield, mp: 112-114 °C, ^{1}H-NMR (600 MHz, DMSO-d6): δ 2.24 (s, 3H), 2.49 (s, 3H), 2.53 (s, 3H), 6.28 (s, 1H), 7.24 (t, *J* = 6 Hz, 1H), 7.34 (d, *J* = 6 Hz, 1H), 7.69 (d, *J* = 6 Hz, 1H), 8.30 (s, 1H). ^{13}C NMR (150 MHz, DMSO-d6) δ 14.1, 14.6, 15.2, 112.0, 120.6, 122.0, 122.2, 124.6, 127.0, 129.5, 145.4, 145.8, 153.2, 154.6, 157.3. MS, *m/z*: 255.1 $[M+1]^+$. Anal. Calcd for $C_{15}H_{14}N_2O_2$: C, 70.85; H, 5.55; N, 11.02. Found: C, 70.98; H, 5.53; N, 11.14%.

(3,5-Dimethyl-1*H*-pyrazol-1-yl)(6-methoxybenzofuran-2-yl)methanone (**11h**). Off-white solid, 82% yield, mp: 111-114 °C, ^{1}H-NMR (600 MHz, DMSO-d6): δ 2.23 (s, 3H), 2.51 (s, 3H), 3.82 (s, 3H), 6.25 (s, 1H), 6.95-6.97 (m, 1H), 7.31 (s, 1H), 7.74 (d, *J* = 6 Hz, 1H), 8.25 (s, 1H). ^{13}C NMR (150 MHz, DMSO-d6) δ 14.1, 14.6, 56.3, 96.0, 111.8, 114.9, 120.6, 120.9, 124.9, 145.3, 145.4, 152.9, 157.1, 157.2, 161.4. MS, *m/z*: 271.0 $[M+1]^+$. Anal. Calcd for $C_{15}H_{14}N_2O_3$, C, 66.66; H, 5.22; N, 10.36. Found: C, 66.32; H, 5.20; N, 10.16%.

(6-Bromobenzofuran-2-yl)(3,5-dimethyl-1H-pyrazol-1-yl)methanone (**11i)**. Off-white solid, 78% yield, mp: 104-106 °C, ^{1}H-NMR (600 MHz, DMSO-d6): δ 2.23 (s, 3H), 2.52 (s, 3H), 6.28 (s, 1H), 7.52 (d, *J* = 12 Hz, 1H), 7.84 (d, *J* = 12 Hz, 1H), 8.08 (s,1H), 8.30 (s, 1H). ^{13}C NMR (150 MHz, DMSO-d6) δ 14.1, 14.6, 112.1, 115.8, 120.0, 121.8, 126.1, 126.8, 127.9, 145.5, 146.7, 153.4, 155.6, 156.9. MS, *m/z*: 318.9 $[M^+]$. Anal. Calcd for $C_{14}H_{11}BrN_2O_2$: C, 52.69; H, 3.47; N, 8.78. Found: C, 52.43; H, 3.73; N, 8.54%.

(3,5-dimethyl-1*H*-pyrazol-1-yl)(5-nitrobenzofuran-2-yl)methanone (11j). Brown solid, 56% yield, mp: 155-157 °C, ^{1}H-NMR (400 MHz, $CDCl_3$): δ 2.33 (s, 3H), 2.65 (s, 3H), 6.09 (s, 1H), 7.73 (d, *J* = 12 Hz, 1H), 8.36-8.39 (m, 1H), 8.48 (s, 1H), 8.70 (d, *J* = 4 Hz, 1H). ^{13}C NMR (100 MHz, $CDCl_3$) δ 13.9, 14.5, 111.7, 112.9, 119.6, 120.2, 122.8, 127.6, 144.7, 145.8, 149.0, 153.7, 156.7, 157.8. MS, *m/z*: 287.1 $[M+2]^+$. Anal. Calcd for $C_{14}H_{11}N_3O_4$: C, 58.95; H, 3.89; N, 14.73. Found: C, 58.73; H, 3.84; N, 14.54%.

Molecular docking analysis

All of the synthesized substituted benzofuran-pyrazole hybrids were evaluated for molecular docking analysis against NS5A and NS5B proteins of HCV. The crystal structure of both proteins of HCV were obtained from Protein Data Bank with PDB IDs i.e., 3FQM and 3MWW for NS5A and NS5B targets, respectively[47,48]. These proteins were employed as receptors for induced fit docking to determine the potential of synthesized hybrids as anti-HCV agents. Molecular docking analysis was performed by using AutoDockTools 1.5.7[49]. The search grid was set to center_x: 23.078, center_y: 8.687 and center_z: 11.871 for NS5A protein and to center_x: -24.999, center_y: 25.175 and center_z: 8.47 for NS5B protein with dimensions size_x: 40, size_y: 40 and size_z: 40 for both receptors. For each compound, pose with low docking score was selected and BIOVIA Discovery Studio 2024 was employed to visualize the respective ligand-protein interactions.

ADMET analysis

The ADMET analysis of newly synthesized potent hybrids and standard inhibitors was performed by using ADMElab 3.0[50]. The required smiles of the selected compounds were extracted from ChemDraw and the

obtained SMILES were then pasted in the online software to determine the physiochemical, medicinal, metabolism, distribution, absorption, excretion and toxicity features of these selected compounds.

Acknowledgements

Facilities provided by Government College University Faisalabad, Pakistan are greatly acknowledged.

Supplementary Material

The characterized spectra (^{1}H-NMR & ^{13}C-NMR), along with supporting molecular docking interaction tables and figures have been provided in the supplementary file attached with this manuscript.

References

1. Makhova, N. N.; Belen'kii, L. I.; Gazieva, G. A.; Dalinger, I. L.; Konstantinova, L. S.; Kuznetsov, V. V.; Kravchenko, A. N.; Krayushkin, M. M.; Rakitin, O. A.; Starosotnikov, A. M.; Fershtat, L. L.; Shevelev, S. A.; Shirinian, V. Z.; Yarovenko, V. N. *Russ. Chem. Rev.* **2020**, *89*, 55. https://doi.org/10.1070/RCR4914
2. Ebenezer, O.; Jordaan, M. A.; Carena, G.; Bono, T.; Shapi, M.; Tuszynski, J. A. *Int. J. Mol. Sci*. **2002**, *23*, 8117. https://doi.org/10.3390/ijms23158117
3. Havrylyuk, D.; Roman, O.; Lesyk, R. *Eur. J. Med. Chem.* **2016**, *111*, 145. https://doi.org/10.1016/j.ejmech.2016.02.030
4. Kumari, K.; Raghuvanshi, D. S.; Jouikov, V.; Singh, K. N. *Tetrahedron Lett.* **2012**, *53*, 1110. https://doi.org/10.1016/j.tetlet.2011.12.094
5. Kumara, K.; Kumar, A. D.; Naveen, S.; Kumar, K. A.; Lokanath, N. K. *J. Mol. Struct.* **2018**, *1161*, 285.
6. Clapham, K. M.; Batsanov, A. S.; Bryce, M. R.; Tarbit, B. *Org. Biomol. Chem.* **2009**, *7*, 2155. https://doi.org/10.1039/b901024f
7. Aleem, M. A. E.; El-Remaily, A. A. *Tetrahedron* **2014**, *70*, 2971. https://doi.org/10.1016/j.tet.2014.03.024
8. Bihani, M.; Bora, P. P.; Bez, G.; Askari, H. *ACS Sustain. Chem. Eng*. **2011**, *1*, 440. https://doi.org/10.1021/sc300173z
9. Bhosle, M. R.; Khillare, L. D.; Dhumal, S. T.; Mane, R. A. *Chin. Chem. Lett*. **2016**, 27, 370. https://doi.org/10.1016/j.cclet.2015.12.005
10. Waghmare, A. S.; Pandit, S. S. *J. Saudi Chem. Soc.* **2017**, 21, 286. https://doi.org/10.1016/j.jscs.2015.06.010
11. Babaie, M.; Sheibani, H. *Arab. J. Chem.* **2014**, *4*, 159. https://doi.org/10.1016/j.arabjc.2010.06.032
12. Chaudhari, M. A.; Gujar, J. B.; Kawade, D. S.; Shingare, M. S. *Chem. Bio Interface*. **2015**, *5*, 44.
13. Wang, C.; Jiang, Y. H.; Yan, C. G. *Chem. Lett.* **2015**, *26*, 889.

14. Kiyani, H.; Samimi, H. A.; Ghorbani, F.; Esmaielia, S. *Curr. Chem. Lett.* **2011**, *2*, 197.
15. Vafajooa, Z.; Hazeria, N.; Maghsoodloua, M. T.; Veisib, H. *Chin. Chem. Lett.* **2015**, *26*, 973.
16. Karimi-Jaberi, Z.; Shams, M. M. R.; Pooladian, B. *Acta Chim. Slov.* **2011**, *60*, 105.
17. Zolfigol, M. A.; Tavasoli, M.; Moosavi-Zare, A. Z.; Moosavi, P.; Kruger, H.G.; Shiri, M.; Khakyzadeh, V. *RSC Adv*. **2011**, *3*, 25681. https://doi.org/10.1039/c3ra45289a
18. Khazdooz, L.; Zarei, A. *Irani J. Catal.* **2016**, *6*, 69.
19. Ambethkar, S.; Padmini, V.; Bhuvanesh, N.J. *J. Adv. Res.* **2015**, *6*, 975. https://doi.org/10.1016/j.jare.2014.11.011
20. Kshirsagar, S. W.; Patil, N. R.; Samant, S. D. *Synth. Commun.* **2011**, *41*, 1120.
21. Nemati, F.; Nikkhah, S. H.; Elhampour, A. *Chin. Chem. Lett*. **2015**, *26*, 1197. https://doi.org/10.1016/j.cclet.2015.07.009
22. Wang, Z.; Qin, H. *Green Chem.* **2004**, *6*, 90. https://doi.org/10.1039/b312833d
23. Polshettiwar, V.; Varma, R. S. *Tetrahedron Lett.* **2008**, *49*, 397. https://doi.org/10.1016/j.tetlet.2007.11.017
24. Milovanović, V.; Petrović, Z. D.; Novaković, S.; Bogdanović, G. A.; SimiJonović, D.; Petrović, V. P. *J. Mol. Struct.* **2019**, *1195*, 85. https://doi.org/10.1016/j.molstruc.2019.05.095
25. Chen, X., She, J., Shang, Z. C., Wu, J.; Zhang, P. *Synth. Commun.* **2009**, *39*, 947. https://doi.org/10.1080/00397910802441551
26. Genin, M. J.; Biles, C.; Keiser, B. J.; Poppe, S. M.; Swaney, S. M.; Tarpley, W. G.; Yagi, Y.; Romero, D. L. *J. Med. Chem*. **2000**, *43*, 1034. https://doi.org/10.1021/jm990383f
27. Yu, B.; Zhou, S.; Cao, L.; Hao, Z.; Yang, D.; Guo, X.; Zhang, N.; Bakulev, V. A.; Fan, Z. *J. Agric. Food Chem*. **2020**, *68*, 7093. https://doi.org/10.1021/acs.jafc.0c00062
28. Chauhan, S.; Paliwal, S.; Chauhan, R. *Commun.* **2014**, *44*, 1333-1374. https://doi.org/10.1080/00397911.2013.837186
29. Verma, R.; Verma, S. K.; Rakesh, K. P; Girish, Y. R.; Ashrafizadeh, M.; Kumar, K. S. S.; Rangappa, K. S. *Eur. J. Med. Chem.* **2021**, *212*, 113134. https://doi.org/10.1016/j.ejmech.2020.113134
30. Taher, A. T.; Sarg, M.T.M.; Ali, N. R. E.; Elnagdi, N. H. *Bioorg. Chem.* **2019**, *89*, 103023. https://doi.org/10.1016/j.bioorg.2019.103023
31. Szabo, G.; Fischer, J.; Kis-Varga, A.; Gyires, K. *J. Med. Chem.* **2008**, *51*, 142. https://doi.org/10.1021/jm070821f
32. Lusardi, M.; Spallarossa, A.; Brullo, C. *Int. J. of Mol. Sci.*, **2023,** *24*, 7834. https://doi.org/10.3390/ijms24097834
33. Xu, Z.; Zhao, S.; Lv, Z.; Feng, L.; Wang, Y.; Zhang, F.; Bai, L.; Deng, J. *Eur. J. Med. Chem.* **2019**, *162*, 266. https://doi.org/10.1016/j.ejmech.2018.11.025
34. Irfan, A.; Faiz, S.; Rasul, A.; Zafar, R.; Zahoor, A. F.; Kotwica-Mojzych, K.; Mojzych, M. *Molecules* **2022**, *27*, 1023.

https://doi.org/10.3390/molecules27031023
35. Irfan, A.; Faisal, S.; Zahoor, A. F.; Noreen, R.; Al-Hussain, S. A.; Tuzun, B.; Javaid, R.; Elhenawy, A. A.; Zaki, M. E. A.; Ahmad, S.; Abdellattif, M. H. *Pharmaceuticals* **2023**, *16*, 829. https://doi.org/10.3390/ph16060829
36. Carlsson, B.; Singh, B. N.; Temciuc, M.; Nilsson, S.; Li, Y. L.; Mellin, C.; Malm, J. *J. Med. Chem.* **2002**, *45,* 623. https://doi.org/10.1021/jm001126+
37. Irfan, A.; Faisal, S.; Ahmad, S.; Saif, M. J.; Zahoor, A. F.; Khan, S. G.; Javid, J.; Al-Hussain, A.; Muhammed, M. T.; Zaki, M. E. *Biomedicines* **2023**, *11,* 3085. https://doi.org/10.3390/biomedicines11113085
38. Irfan, A.; Faisal, S.; Ahmad, S.; Al-Hussain, S. A.; Javed, S.; Zahoor, A. F.; Parveen, B.; Zaki, *Pharmaceuticals* **2023**, *16*, 344. https://doi.org/10.3390/ph16030344
39. Mushtaq, A.; Ahmad, M. N.; Zahoor, A. F.; Kamal, S.; Ali, K. G.; Javid, J.; Parveen, B.; Nazeer, U.; Bhat, M. A. *RSC Adv.* **2024**, *14*, 37521. https://doi.org/10.1039/D4RA05649C
40. Nevagi, R. J.; Dighe, S. N.; Dighe, S. N. *Eur. J. Med. Chem.* **2015**, *97*, 561. https://doi.org/10.1016/j.ejmech.2014.10.085
41. Abd El-Karim, S. S.; Mahmoud, A. H.; Al-Mokaddem, A. K.; Ibrahim, N. E.; Alkahtani, H. M., Zen, A. A.; Anwar, M. M. *Molecules* **2023**, *28*, 6814. https://doi.org/10.3390/molecules28196814
42. Abd El-Karim, S. S.; Anwar, M. M.; Syam, Y. M.; Awad, H. M.; El-Dein, A. N.; El-Ashrey, M. K.; Alkahtani, H. M.; Abdelwahed, S. H. *Pharmaceuticals* **2024**, *17*, 1664. https://doi.org/10.3390/ph17121664
43. Azimi, F.; Azizian, H.; Najafi, M.; Khodarahmi, G.; Saghaei, L.; Hassanzadeh, M.; Ghasemi J. B.; Faramarzi, M. A.; Larijani, B.; Hassanzadeh, F.; Mahdavi, M. *Sci. Rep.* **2021**, *11*, 20776. https://doi.org/10.1038/s41598-021-99899-1
44. Faiz, S.; Zahoor, A. F.; Ajmal, M.; Kamal, S.; Ahmad, S.; Abdelgawad, A. M.; Elnaggar, M. E. *J. Heterocycl. Chem.* **2019**, *56*, 2839. https://doi.org/10.1002/jhet.3674
45. Reyes, G. R. *J. Biomed. Sci.* **2002**, *9*, 187. https://doi.org/10.1007/BF02256065
46. Ishii, K.; Tanaka, Y.; Yap, C. C.; Aizaki, H.; Matsuura, Y.; Miyamura, T. *Hepatol.* **1999**, *29*, 1227. https://doi.org/10.1002/hep.510290448
47. Brice Landry, K.; Tariq, S.; Malik, A.; Sufyan, M.; Ashfaq, U. A.; IJaz, B.; Shahid, A. A. *J. Biomol. Struct. Dyn.* **2022**, *40*, 7829. https://doi.org/10.1080/07391102.2021.1902395
48. Dhanasekaran, S.; Selvadoss, P. P.; Manoharan, S. S.; Jeyabalan, S.; Yaraguppi, D. A.; Choudhury, A. A.; Rajeswari, V. D.; Ramanathan, T.; Sekar, M.; Subramaniyan, V.; Shing, W. L. *Cell Biochem. Biophys.* **2024**, *82*, 2473. https://doi.org/10.1007/s12013-024-01359-w

49. Wang, G.; Peng, Z.; Wang, J.; Li, X.; Li, J. *Eur. J. Med. Chem.* **2017**, *125*, 423. https://doi.org/10.1016/j.ejmech.2016.09.067

50. Fu, L.; Shi, S.; Yi, J.; Wang, N.; He, Y.; Wu, Z.; Peng, J.; Deng, Y.; Wang, W.; Wu, C.; Lyu, A.; Zeng, X.; Zhao, W.; Hou, T.; Cao, D. *Nucleic Acids Res.* **2024,** *52*, W422. https://doi.org/10.1093/nar/gkae236